

# Deletion of *PREPL*, a Gene Encoding a Putative Serine Oligopeptidase, in Patients with Hypotonia-Cystinuria Syndrome

Jaak Jaeken,<sup>1,\*</sup> Kevin Martens,<sup>2,3,\*</sup> Inge François,<sup>1</sup> François Eyskens,<sup>5</sup> Claudine Lecointre,<sup>6</sup> Rita Derua,<sup>4</sup> Sandra Meulemans,<sup>2</sup> Jerry W. Slootstra,<sup>7</sup> Etienne Waelkens,<sup>4</sup> Francis de Zegher,<sup>1</sup> John W. M. Creemers,<sup>2</sup> and Gert Matthijs<sup>3</sup>

<sup>1</sup>Department of Paediatrics, University Hospitals Leuven, <sup>2</sup>Laboratory for Molecular Cell Biology, Department for Human Genetics, University of Leuven and Flanders Interuniversity Institute for Biotechnology, and <sup>3</sup>Laboratory for Molecular Diagnosis, Department for Human Genetics, and <sup>4</sup>Department of Biochemistry, University of Leuven, Leuven, Belgium; <sup>5</sup>Department of Paediatrics, University of Antwerp, Antwerp; <sup>6</sup>Department of Paediatrics, University of Rouen, Rouen, France; and <sup>7</sup>PEPSCAN Systems, Lelystad, The Netherlands

In 11 patients with a recessive congenital disorder, which we refer to as “the hypotonia-cystinuria syndrome,” microdeletion of part of the *SLC3A1* and *PREPL* genes on chromosome 2p21 was found. Patients present with generalized hypotonia at birth, nephrolithiasis, growth hormone deficiency, minor facial dysmorphism, and failure to thrive, followed by hyperphagia and rapid weight gain in late childhood. Since loss-of-function mutations in *SLC3A1* are known to cause isolated cystinuria type I, and since the expression of the flanking genes, *C2orf34* and *PPM1B*, was normal, the extended phenotype can be attributed to the deletion of *PREPL*. *PREPL* is localized in the cytosol and shows homology with prolyl endopeptidase and oligopeptidase B. Substitution of the predicted catalytic residues (Ser470, Asp556, and His601) by alanines resulted in loss of reactivity with a serine hydrolase-specific probe. In sharp contrast to prolyl oligopeptidase and oligopeptidase B, which require both aminoterminal and carboxyterminal sequences for activity, *PREPL* activity appears to depend only on the carboxyterminal domain. Taken together, these results suggest that *PREPL* is a novel oligopeptidase, with unique structural and functional characteristics, involved in hypotonia-cystinuria syndrome.

The prolyl oligopeptidase family (SC clan, family S9) (Rawlings and Barrett 1994) represents a class of serine peptidases that are selective for small peptides (generally <30 aa) (Polgar 2002). The four main members are prolyl endopeptidase (PREP) (EC 3.4.21.26; MIM 600400), oligopeptidase B (OpdB) (EC 3.4.21.83), dipeptidyl-peptidase IV (DPPIV) (EC 3.4.14.5; MIM 102720), and acylaminoacyl-peptidase (APEH) (EC 3.4.19.1; MIM 102645) (Polgar 2002). PREP and OpdB are endopeptidases that cleave carboxyterminal of proline and arginine/lysine residues, respectively. DPPIV and APEH, on the other hand, are exopeptidases. The former is specific for proline at the penultimate position, and the latter removes acylated aminoterminal amino acids from blocked peptides (Polgar 2002).

The family has a conserved domain structure, with a  $\beta$ -propeller domain preceding the catalytic domain. The catalytic triad residues are located in a specific order (Ser, Asp, His) and in conserved places (Ollis et al. 1992; Nardini and Dijkstra 1999). The structural basis for selectivity for small peptides is the  $\beta$ -propeller, which acts as a gating filter whose central tunnel excludes large, structured peptides (Fulop et al. 2000), although this concept has recently been challenged (Juhasz et al. 2005).

All four enzymes have been implicated in clinical conditions and are potential therapeutic targets. Serum PREP activity is increased in patients with mania and schizophrenia (Maes et al. 1995) but decreased in patients with different stages of depression (Maes et al. 1994). Recent studies indicate that PREP is involved in the regulation of the inositol (1,4,5)-triphosphate pathway—the same pathway that is affected by lithium, which is often used as a therapeutic agent for the treatment of depression (Williams et al. 1999, 2002; Schulz et al. 2002). OpdB plays a crucial role in the host cell invasion by the protozoan parasite *Trypanosoma cruzi* in Chagas disease, and deletion of the gene results in greatly reduced cell invasion capacity. OpdB generates an active  $Ca^{2+}$  agonist from a cytosolic precursor molecule, which results in the recruitment and fusion of host cell lysosomes at the site of parasite attachment (Burleigh et al. 1997; Caler et al. 1998, 2000). DPPIV inactivates glucagon-like peptide-1 and gastric inhibitory polypeptide, both of which stimulate insulin release. Inhibiting DPPIV is a promising strategy in the treatment of diabetes type 2 (Drucker 2001; Vilsboll et al. 2001). Finally, APEH is deleted in a number of small-cell lung carcinoma cell lines, and it has been suggested that the accumulation of acetylated peptide growth factors could

Received August 29, 2005; accepted for publication October 6, 2005; electronically published November 23, 2005.

Address for correspondence and reprints: Dr. John Creemers, Laboratory for Molecular Cell Biology, Department for Human Genetics, University of Leuven/V.I.B. Gasthuisberg O/N 6, Box 602, Herestraat 49, B-3000 Leuven, Belgium. E-mail: John.Creemers@med.kuleuven.be

\* These authors contributed equally to this work.

*Am. J. Hum. Genet.* 2006;78:38–51. © 2005 by The American Society of Human Genetics. All rights reserved. 0002-9297/2006/7801-0006\$15.00

contribute to tumor cell proliferation (Scaloni et al. 1992).

Recently, a 179-kb deletion (2p21 deletion syndrome) (MIM 606407) containing at least four genes (*SLC3A1*, *PREPL*, *PP2C $\beta$* , and *C2orf34*) was found in seven patients in a small Bedouin clan (Parvari et al. 2001). One of the genes was found to be homologous to *PREP* and was, therefore, named “prolyl oligopeptidase-like” (*PREPL*). The contribution of *PREPL* to the severe syndrome, which is characterized by cystinuria type I, hypotonia, neonatal seizures, severe mental retardation, different facial dysmorphism, and mitochondrial dysfunction, could not be established (Parvari et al. 2005).

Here we report a novel syndrome characterized by hypotonia and cystinuria type I. This hypotonia-cystinuria syndrome (HCS) is caused by a microdeletion of only two genes, *SLC3A1* and *PREPL*. The former encodes the heavy-chain subunit of the cystine and dibasic amino acid transporter localized in the renal proximal tubule and small intestine (Goodyer et al. 2000). Inactivation of this gene product is known to cause isolated cystinuria type I (Calonge et al. 1994; Font-Llitjos et al. 2005) (MIM 220100). The other clinical features of the syndrome can, therefore, be attributed to the gene product of *PREPL*.

## Methods

### Patients

Patients were studied after informed consent was obtained. They all presented with hypotonia and feeding difficulties from birth and were referred to us between the ages of 2 wk and 7 mo.

### Genomic PCR

The initial semiquantitative PCR analysis of the *SLC3A1* locus was performed as described elsewhere (Purroy et al. 2000). For new amplicons, primers were designed using Primer3 and sequences available in GenBank. PCR products were amplified using 150 ng of genomic DNA, by use of either the PCR Master Mix (Promega) or the Expand Long Template PCR System (Roche Molecular Biochemicals). Junction fragments were purified with the Montage PCR Centrifugal Filter Device (Millipore) before sequencing. All primer sequences and annealing temperatures are available on request. Primer sequences for the microsatellites were obtained from the GDB Human Genome Database.

### Quantitative RT-PCR

RNA from Epstein Barr virus (EBV)-transformed leukocytes was extracted using the QIAquick RNA extraction kit (Qiagen), in accordance with the manufacturer's protocol. One microgram of RNA was DNase (Fermentas) treated before cDNA synthesis with SuperScript II (Invitrogen). cDNA was diluted four times for analysis. Quantitative PCR was performed using qPCR MasterMix for SYBR Green I detection

(Eurogentec) on the ABI7000 sodium dodecyl sulphate (SDS) system (Applied Biosystems), in accordance with the manufacturer's guidelines. Primers were developed with Primer-Express software (Applied Biosystems).

### In Silico Analysis

Sequences (EST and homologues) were obtained via BLAST searches. Multiple sequence alignments were performed using ClustalW. Subcellular localization was predicted using the PSORT II program. Secondary structure predictions were performed using PredictProtein and JPRED.

### Northern Blotting

A human multiple-tissue northern blot (Clontech Laboratories) was hybridized in accordance with the manufacturer's protocol. A 1-kb cDNA fragment spanning exons 2–8 was used as a probe.

### Eukaryotic Expression Constructs

Human *PREPL<sub>s</sub>* cDNA (GenBank accession number AB007896) was obtained from the Kazusa DNA Research Institute (Kikuno et al. 2004). Porcine PREP was provided by L. Polgar (Szeltner et al. 2000). OpdB was PCR amplified using DNA from the *Escherichia coli* K12 strain (GenBank accession number U00096) as a template. All cDNAs, including those encoding mutated and truncated proteins, were subcloned into a pcDNA3.1 expression vector (Invitrogen) introducing an aminoterminal FLAG epitope tag (DYKDDDDK). All constructs and mutations were confirmed by cycle sequencing (Applied Biosystems).

### Site-Directed Mutagenesis

Active site mutants were generated using a QuikChange site-directed mutagenesis kit (Stratagene), in accordance with the guidelines of the supplier. Truncated mutants encoding only the carboxyterminal catalytic domain (*PREPL* aa 342–638, OpdB aa 405–687, and PREP aa 426–710) were generated by PCR and cloned in pcDNA3.1.

### Immunopurification

HEK293T cells were transiently transfected with the indicated plasmid with the use of Fugene6 (Roche Molecular Biochemicals). After 24 h of incubation, cells were washed twice with PBS and were harvested by scraping in ice-cold PBS. Cells were lysed by 10 passages through a 26-gauge needle. Cell debris was removed by centrifugation (10,000 g at 4°C for 10 min). FLAG-tagged recombinant protein was immunopurified from precleared lysate by use of preformed complexes of anti-FLAG M2 antibody (Sigma-Aldrich) and protein G Sepharose (GE Healthcare), as described elsewhere (Jackson et al. 2003).

### Bacterial Expression and Purification

Human *PREPL<sub>s</sub>* cDNA was subcloned in the pQE9 expression vector (Qiagen) with an aminoterminal His epitope. At 30°C, 250-ml cultures of *E. coli* strain M15 (*PREP<sub>4</sub>*) were

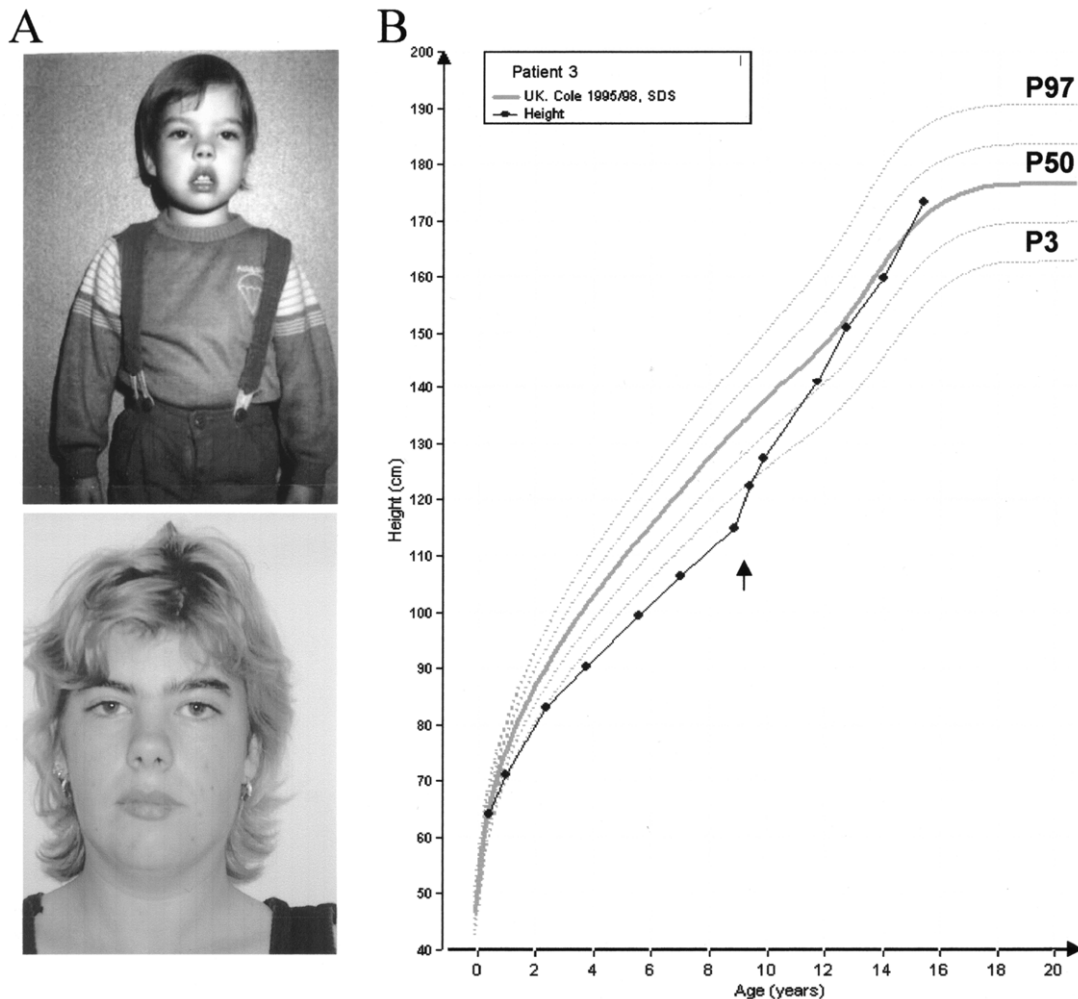


**Figure 1** Clinical presentation of HCS. A, Patient 5-I during childhood (*top*) and adulthood (*bottom*). B, Growth curve of patient 3-I, illustrating the excellent response to growth hormone treatment. Vertical arrow indicates the age at which the treatment was started.

grown overnight, and expression was induced by the use of 1-mM isopropyl- $\beta$ -D-thiogalactopyranoside.

Bacterial pellets were resuspended in 100 ml of 50-mM Tris buffer (pH 8) and were lysed by the addition of 0.1 mg/ml lysozyme (30 min at 4°C), followed by sonication. Cleared lysates (10 min at 10,000 g) were purified on the AKTA explorer (GE Healthcare) with the use of a Ni-NTA affinity column (Sigma). PREPL<sub>s</sub> was eluted with imidazole (Merck), at a concentration of 100 mM. Bacterially produced PREPL<sub>s</sub> was used for inhibitor profiling.

#### Reaction with Fluorophosphate-Biotin

Fluorophosphate-biotin (FP-biotin) was synthesized as described elsewhere (Liu et al. 1999). Immunopurified proteins were resolved in 19.5  $\mu$ l of a 50-mM phosphate buffer at pH 8. FP-biotin (200  $\mu$ M in dimethyl sulfoxide) was added to a final concentration of 5  $\mu$ M, and the reaction mixture was incubated at 37°C for 30 min. Reactions were quenched by

the addition of SDS-PAGE loading buffer (reducing) and heating at 95°C for 10 min.

Competition experiments were performed in a total volume of 40  $\mu$ l with the use of 1  $\mu$ g of bacterially expressed PREPL<sub>s</sub> spiked with 250 ng of FLAG M2 for normalization purposes, as explained below. PREPL<sub>s</sub> was preincubated in the presence or absence of inhibitor for 15 min at 37°C, followed by a reaction with FP-biotin for 15 min. Reactions were stopped by the addition of SDS-PAGE loading buffer (reducing) and heating at 95°C for 10 min.

#### Detection of FP-Biotin Reactivity

The reactions were run on SDS-PAGE and were transferred by electroblotting on to a nitrocellulose membrane, as described elsewhere (Roebroek et al. 2004). Blots were incubated with horseradish peroxidase-conjugated streptavidin (Dako), were visualized by Western Lightning Chemiluminescence Reagent Plus (Perkin Elmer Life Sciences), and were exposed with

**Table 1****Neonatal and Relevant Endocrinological Data on the Patients**

Patient	Sex	Birth Weight (g)	Birth Length (cm)	Gestational Period (wk) <sup>a</sup>	Delivery Method <sup>b</sup>	Peak GH ( $\mu\text{g/liter}$ )	IGF-1 (SD score)	Age at Puberty (years) <sup>c</sup>	FSH (U/liter) <sup>d</sup>
1-I	M	2,600	44	36	CS (breech)	>10	-2.3	<9	NA <sup>e</sup>
2-I	M	3,510	50.5	41	Induction	NA	NA	<9	NA <sup>e</sup>
8-I	M	3,970	52	41	NL	6.6	-1.8	NA	NL
3-I	M	3,600	50	40	CS (breech)	7.3	-4.8	13.1	NL
7-I	M	2,800	49	40	Induction	5	-3.7	13.4	16.6 <sup>f</sup>
6-I	M	3,500	NA	NA	NA	NA	NA	NA	NA
7-II	F	2,890	NA	40	NL	>10	-2.8	12.5	22.8 <sup>g</sup>
4-I	F	3,250	52	40	CS	6	-2.6	13.7	52.8
8-II	F	2,880	49	41	NL	2	-3.1	Primary amenorrhea	76
9-I	F	3,450	51	41	NL	<2	-3.7	15	NA
5-I	F	1,900	NA	NA	NA	NA	NA	15	NL

NOTE.—NL = normal. NA = not available.

<sup>a</sup> Weeks of pregnancy, counting from mother's last menstruation.

<sup>b</sup> CS = cesarean section.

<sup>c</sup> For males, age at which testes >4 ml. For females, age at menarche.

<sup>d</sup> FSH normal values <10 U/liter.

<sup>e</sup> Age <9 years.

<sup>f</sup> Orchidopexy at age 5 years.

<sup>g</sup> Premenarcheal, regular menses.

Super RX medical x-ray film (Fuji). The expression of recombinant protein was subsequently confirmed on the same blot with the use of biotinylated anti-FLAG M2 antibody.

In the competition experiments, the FLAG M2 antibody was detected by the incubation of the lower part of the blot with horseradish peroxidase-conjugated rabbit antimouse antiserum (Dako). Chemiluminescence signals of both FP-biotin and FLAG M2 were quantified using the Kodak Image Station 440C (Perkin Elmer Life Sciences). The FLAG M2 signal was used for normalization.

#### Immunocytochemistry

Chinese hamster ovary (CHO)-K1 cells were transfected as described elsewhere (Creemers et al. 2000) and were analyzed 24 h later. Immunocytochemistry was performed essentially as described elsewhere (Creemers et al. 1996), except that the cells were washed and fixed for 5 min in methanol at  $-20^{\circ}\text{C}$ . Slides were analyzed on a Zeiss Axiophot fluorescence microscope equipped with an RT slider SPOT CCD camera (Diagnostic Instruments) that used SPOT RT software.

#### Activity Studies

Substrate specificity of PREPL was tested using fluorogenic substrates (peptidyl 4-methyl-7 coumarylamide [Bachem]). Immunopurified proteins were resuspended in  $95\ \mu\text{l}$  of reaction buffer (50-mM phosphate buffer at pH 8, 10-mM EDTA, and 2-mM dithiothreitol) and were preincubated at  $37^{\circ}\text{C}$  for 5 min. Substrate was added at a final concentration of  $200\ \mu\text{M}$ . Fluorogenic leaving groups were detected in real time, by use of a FLUOstar Galaxy (BMG Labtechnologies) spectrofluorimeter, at excitation and emission wavelengths of 390 nm and 420 nm, respectively.

## Results

### Hypotonia-Cystinuria Syndrome

Eleven patients (six male and five female) from nine families were studied. Seven of the nine families were Flemish (from Antwerp, Belgium) and two were French (from Normandy, France). Although the Flemish patients lived within an area of only  $80\ \text{km} \times 20\ \text{km}$ , consanguinity could not be documented between parents. The oldest patient was described with cystinuria, benign myopathy, and dwarfism (Clara and Lowenthal 1966). His three similarly affected siblings were lost to follow-up and were, therefore, not included in this study.

The parents and siblings of nine patients underwent a complete clinical examination and urine amino acid analysis, but no abnormalities were found. The ages of the patients ranged from 4 years to 42 years. Decreased fetal movements were reported in nine patients. Five children were born by cesarean section or induction, and the others had a tendency towards postdatism. Mean birth weight ( $n = 9$ ) was  $-0.77\ \text{SD}$ . All patients showed a generalized hypotonia from birth, with major feeding problems (mainly anorexia) necessitating gavage feeding in three patients and a gastrostomy in one. Failure to thrive persisted up to the ages of 6–8 years, and a period of hyperphagia and rapid weight gain followed.

All showed minor facial dysmorphism, characterized mainly by dolichocephaly and ptosis of the eyelids; the latter improved with age but did not completely disappear (fig. 1A). Tented upper lip was noted in four patients. Thick and/or decreased saliva was reported in



six patients. Gross motor development was mildly to moderately retarded, with unaided walking achieved between the ages of 15 mo and 3 years. Fine motor development was normal. Speech was normal or mildly retarded, but all patients exhibited nasal speech. Of the seven patients older than 6 years, four received normal educations, and the remaining three received special educations.

Epileptic phenomena were not recorded in any of the patients. Impaired growth became evident in eight of nine patients at a median age of 3 years (range 2–6 years), either by decreased growth velocity or by the absence of growth acceleration while rapid weight gain occurred. In six of the eight patients, peak growth hormone levels after two different provocation tests were insufficient. Priming with sex hormone was performed when necessary. Two patients had repeatedly low levels of IGF-1. Growth hormone treatment (25 µg/kg/d) was started in all eight patients at a median age of 10.7 years (range 1.4–13.6 years), with excellent results. The median actual height and height velocity SD score before the start of growth hormone treatment was –2.3 (range –4 to –0.9) and –1.35 (range –2.8 to 0.4), respectively. Median latest height SD score was –0.3 (range –2 to 1.7) and median latest BMI SD score was 1.7 (range 0.5–2.5). A representative growth curve is presented in figure 1B.

There was a tendency towards late puberty in seven of nine patients, four of whom presented hypergonadotropic hypogonadism (range of basal serum follicle stimulating hormone [FSH] 17–76 U/liter) (table 1). Serum dehydroepiandrosterone sulfate levels were low in all children older than 6 years, a finding suggestive of lowered adrenarche. Serum prolactin levels were not elevated.

All patients presented within their first decades with symptomatic nephrolithiasis due to classical cystinuria type I. Further metabolic work-up was normal, including hemograms and tests of blood lactate, pyruvate, glucose, plasma amino acids, serum free and total carnitine, acylcarnitines, creatine kinase, lactate dehydrogenase, insulin, liver function, sialotransferrins, and urinary organic acids.

Electromyography and nerve conduction velocity were normal in all patients. A brain scan or magnetic resonance imaging was performed in seven patients with normal results, except in one patient with a small-sized

anterior pituitary gland. Muscle biopsy performed in three patients (aged 6 mo, 8 mo, and 1 year) did not show any specific abnormality. In particular, there was no histological evidence for mitochondrial disease, and the enzymatic activity of mitochondrial respiratory chain complex I–V was normal. An imprinting defect on chromosome 15 was ruled out by methylation analysis with the use of the KB17 probe (Buiting et al. 1998) (data not shown), excluding Prader-Willi syndrome (PWS).

#### Deletion Screening of the *SLC3A1* Locus

Isolated cystinuria type I is caused by mutations in *SLC3A1* (Calonge et al. 1994). Two siblings were shown elsewhere to be compound heterozygous for deletions in this gene (Purroy et al. 2000). On one allele, exons 2–10 were deleted, whereas on the other, only exon 10 was missing. The *SLC3A1* gene was therefore screened in the remaining nine patients by use of semiquantitative PCR analysis. Deletions were detected in all patients. The presence of the deleted allele was confirmed in the parents, if available. The region proximal to the *SLC3A1* gene was subsequently analyzed to estimate the size of the deletions.

Primers flanking the breakpoint were used to generate junction fragments (fig. 2B and table A1 [online only]). Subsequently, these junction fragments were sequenced to determine the exact breakpoints. In total, four unique deletions were found (fig. 2A). Their sizes range from 23.8 kb to 75.5 kb. The distribution of the different alleles is presented in table 2. The different deletions disrupt the coding regions of only two genes, *SLC3A1* and *PREPL* (*KIAA0436* and *FLJ16627*).

To exclude the possibility that the deletions also affect the two flanking genes—*C2orf34* (*FLJ23451*), located proximal to *PREPL*, and *PPM1B*, located distal to *SLC3A1*—we have analyzed their expression in the EBV-transformed leukocytes of one patient with deletion B. Glyceraldehyde-3-phosphate dehydrogenase (*GAPDH*) expression was used to normalize the data. As is shown in table 3, similar expression levels were observed in patient and controls.

#### Haplotype Analysis

Only four different deletions were found on a total of 18 independent chromosomes. Deletions A, B, C, and D are represented 4, 11, 2, and 1 times, respectively. We

**Figure 2** Genetics of HCS. A, Deletions present in the HCS families. All deletions disrupt the coding sequences of *SLC3A1* and *PREPL*, located on chromosome 2p21. Sizes range from 23.8 kb to 75.5 kb. Sequences flanking the breakpoints are shown and are numbered in accordance with BAC clone 24i5. B, Junction fragments spanning the breakpoint. C, Haplotype analysis for deletion A, B, and C alleles. Dashed lines indicate the breakpoint. Conserved alleles are shaded in gray. For deletion B, the conserved subhaplotypes proximal to the breakpoint are shaded in light gray and dark gray. Families 5 (deletion B/deletion B) and 6 (deletion A/deletion B) are excluded because parents were not available. p= Paternal haplotype; m= maternal haplotype.

**Table 2****Genotypes Present in HCS Families**

Family	Maternal Deletion	Paternal Deletion	Sib Pair	Origin	Reference
1	A	A	No	Belgium	...
2-5	B	B	No	Belgium	...
6	A/B <sup>a</sup>	A/B <sup>a</sup>	No	Belgium	Clara and Lowenthal 1966
7	B	A	Yes	Belgium	Purroy et al. 2000
8	C	C	Yes	France	...
9	D	B	No	France	...

<sup>a</sup> Phase unknown.

examined, using microsatellites and SNPs, whether the first three deletions arose from common ancestors. Five microsatellites (*D2S119*, *D2S2298*, *D2S2174*, *D2S2280*, and *D2S2291*) and 10 SNPs were genotyped. Alleles in linkage disequilibrium were combined into one data point (table A2 [online only]). Conserved haplotypes for markers flanking the breakpoint were found in alleles of deletion A and C. The haplotypes for deletion B can be subdivided into two groups, with a conserved haplotype distal to the breakpoint. Informative haplotypes are shown in figure 2C.

#### In Silico Analysis of PREPL

Analysis of the 5' UTR by use of EST data from the public databases revealed a complex splicing pattern (fig. 3B). Evidence for at least seven splice variants was found with the use of two alternative transcription start sites and two additional exons between the predicted exon 1 and 2 (Parvari et al. 2001), which we have named exons 1A and 1B (fig. 3A and 3B). *PREPL*<sub>3</sub> and *PREPL*<sub>5</sub> use the first transcriptional start, whereas the other isoforms all start 259 bp later. The most prevalent isoforms, *PREPL*<sub>1-4</sub>, splice from exon 1 (at different positions) to exon 2, which harbors the translational start with an inframe stop codon 28 codons upstream of the initiator methionine. This generates the 638-aa short form of the protein (fig. 3A and 3B and fig. 4B), which we refer to as *PREPL*<sub>S</sub>. On the other hand, splice variants *PREPL*<sub>5-7</sub> do not directly splice to exon 2. An inframe start codon is present in exon 1B, which results in a protein with an additional 89 aa and is referred to as *PREPL*<sub>L</sub> (fig. 3A and 3B and fig. 4B). A multiple sequence alignment and clone numbers for the different isoforms can be found in figure A1 (online only) and appendix B (online only).

The 3' UTR contains at least three polyadenylation signals, which all appear to be used on the basis of northern blot analysis and EST clones. Three groups of EST clones were found with a 3' UTR of 2,591 bp, 1,703 bp, and 520 bp (appendix C [online only]). This results in a ubiquitously expressed ~5.1-kb mRNA and tissue-restricted ~4.1-kb (brain) and ~2.8-kb (kidney) tran-

scripts (fig. 3C). Northern blot analysis further revealed a broad tissue distribution of *PREPL*, with the highest expression in brain, heart, kidney, and skeletal muscle.

#### Protein Homology and Secondary Structure Prediction

Orthologues of *PREPL* are found in all vertebrates, with identities ranging from 40% (*Tetraodon nigroviridis*) to 94% (*Mus musculus* and *Rattus norvegicus*) to 99% (*Pan troglodytes*) (calculated for the *PREPL*<sub>S</sub> [fig. 4A]). Orthologous genes are located within syntenic regions of the different species.

BLAST searches revealed homology with *PREP* and *OpdB*, with an overall similarity of 29% and 44%, respectively (fig. 4A and 4B). The crystal structure of *PREP* has been determined and shows two distinct domains, a  $\beta$ -propeller and a catalytic domain. The catalytic domain, which is composed of the aminoterminal 72 aa and the carboxyterminal 283 aa, shows a typical  $\alpha/\beta$ -hydrolase fold (Ollis et al. 1992), and the  $\beta$ -propeller domain is composed of  $\beta$ -sheets (Fulop et al. 1998).

*PREPL*<sub>S</sub> seems to be lacking the aminoterminal component of the catalytic domain. The *PREPL*<sub>L</sub> variant is longer at the amino terminus, but sequence homology with *PREP* and *OpdB* is low. However, secondary structure predictions show similar fold components (fig. 5). Furthermore, in both variants, the last 68 aa of the carboxyterminus share no significant sequence homology, although secondary structure predictions suggest that the  $\alpha/\beta$ -hydrolase fold remains intact (fig. 4B and fig. 5). Moreover, the putative catalytic residues (Ser470 and Asp556) are conserved at the topologically equivalent positions, whereas the catalytic histidine is located in the nonconserved carboxyterminus, most likely His601 or

**Table 3****Expression Analysis of *C2orf34* by Use of Quantitative PCR**

Cycle Threshold	Control 1 (C <sub>t</sub> )	Control 2 (C <sub>t</sub> )	Control 3 (C <sub>t</sub> )	Patient 4-I (C <sub>t</sub> )	Blank (C <sub>t</sub> )
<i>C2orf34</i>	28.65	28.18	28.59	28.59	39.25
PPM1B	27.15	26.91	27.56	27.65	39.54
GAPDH	19.00	19.07	19.30	19.52	35.35

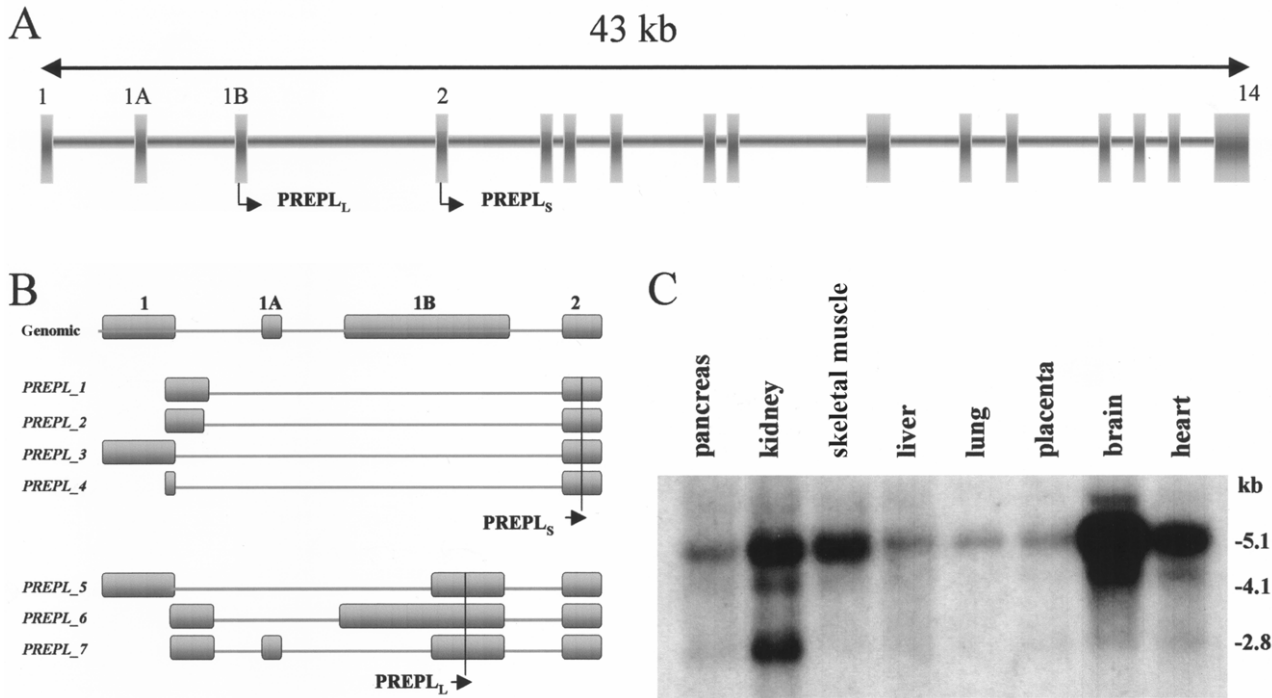


**Figure 3** Expression analysis of *PREPL*. *A*, Genomic organization of *PREPL*. *B*, *In silico* analysis of the 5' UTR revealed two transcriptional start sites. The first transcription start is present in isoforms *PREPL*<sub>3</sub> and *PREPL*<sub>5</sub>, and the second is present in the remaining isoforms. Isoforms *PREPL*<sub>1-4</sub> use the start codon in exon 2, generating a 638-aa protein. *PREPL*<sub>5-7</sub> isoforms contain an additional start site in exon 1B, generating a 727-aa protein. *C*, Human multiple-tissue northern blot shows a broad tissue distribution of a 5.1-kb transcript, with highest expression in brain, kidney, and skeletal muscle. Tissue specific transcripts are present in brain (~4.1 kb) and kidney (~2.8 kb) tissue.

His607. The  $\beta$ -propeller shows relatively low sequence identity. Nevertheless, secondary structure predictions indicate the presence of  $\beta$ -sheets only, which is characteristic for a  $\beta$ -propeller fold (fig. 5).

Structural analysis of PREP and OpdB indicate that the S1 binding pocket is formed by a number of amino acids. In PREP, Trp595 plays a crucial role in aligning the proline (Fulop et al. 1998). In OpdB, on the other hand, Glu576 and Glu578 form a negatively charged pocket, accommodating a basic residue (Gerczei et al. 2000). Multiple alignments with PREP, OpdB, and PREPL show that the equivalent positions in *PREPL*<sub>S</sub> (Glu514 and Glu516) also form a negatively charged pocket, so a basic residue (Arg or Lys) at the P1 position of the substrate (i.e., the first residue aminoterminal of the cleavage site) (Berger and Schechter 1970) is expected (fig. 5).

#### Cellular Localization

The prediction for subcellular localization by use of the PSORT II program is cytosolic (probability 70%) and nuclear (probability 22%) for the *PREPL*<sub>S</sub> isoform. This is the same localization as that for its family members PREP and OpdB. However, the *PREPL*<sub>L</sub> isoform lo-

cation is predicted to be cytoplasmic (probability 39%), nuclear (probability 26%), or mitochondrial (probability 17%). Immunocytochemistry in CHO cells shows cytoplasmic staining for both isoforms. No evidence was found of a nuclear or mitochondrial distribution for the *PREPL*<sub>L</sub> variant (fig. 6A).

#### Substrate Specificity

Substrate specificity of PREPL was tested using substrates typical for PREP (Yoshimoto et al. 1979) and OpdB (Morty et al. 2002). Although all substrates were efficiently cleaved by the corresponding oligopeptidase, no cleavage by PREPL was observed (data not shown). Furthermore, we examined the possibility that PREPL is an aminopeptidase or aminodipeptidylpeptidase with a proline or arginine preference (data not shown). Again, no activity was detected.

#### Activity Profiling

Experimental evidence for serine hydrolase activity was provided using FP-biotin (Liu et al. 1999), a biotinylated derivative from the serine hydrolase inhibitor diisopropylfluorophosphate (DFP). FP-biotin binds covalently to the active site serine only if it resides in a

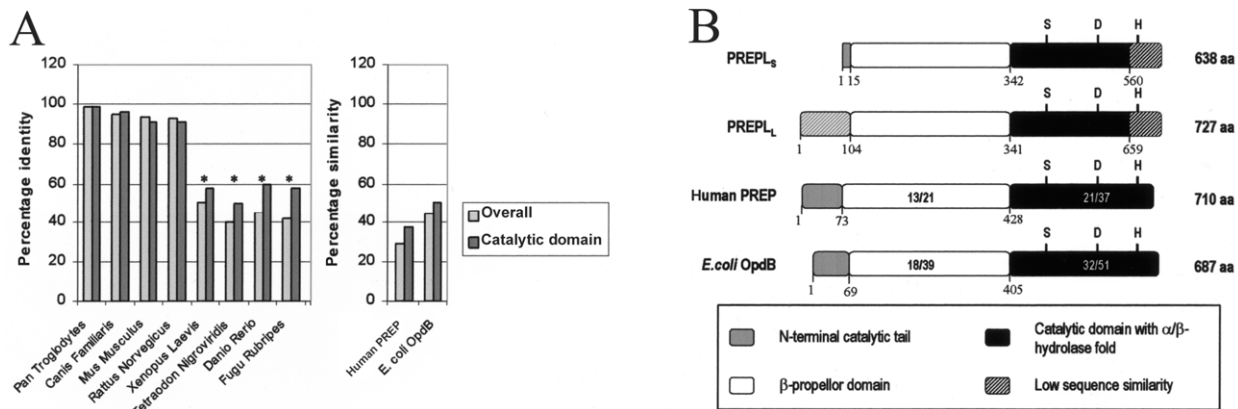


**Figure 4** The PREPL homologues. *A*, Amino acid identity of different PREPL<sub>S</sub> orthologues and amino acid similarity of different PREPL<sub>S</sub> homologues. The light-gray and dark-gray bars represent the identity (*left panel*) or similarity (*right panel*) percentages of the complete sequence and catalytic domain, respectively. An asterisk indicates an incomplete amino acid sequence present in the database. *B*, Schematic representation of the domain structure of the PREPL isoforms. Identity/similarity percentages of the different domains with PREP and OpdB are shown.

catalytically active conformation. As shown in figure 6*B*, FP-biotin reacts with epitope-tagged recombinant PREPL<sub>S</sub> and PREPL<sub>L</sub> but not with PREPL<sub>S</sub> mutants in which a putative catalytic triad residue has been replaced by an alanine residue (fig. 6*C*). The reaction of mutant His607Ala was similar to wild type, whereas the mutation of His601 completely abolished reactivity, identifying His601 as a genuine catalytic residue.

Since all components of the α/β-hydrolase fold are present in the carboxyterminal part of the catalytic domain, we used the activity-based probe to test the folding of this domain in the absence of the propeller domain and aminoterminal component of the catalytic domain. Wild-type PREPL<sub>S</sub>, PREP, and OpdB react with FP-biotin, whereas only the isolated catalytic domain of PREPL reacts with FP-biotin (fig. 6*D*).

FP-biotin can also be used to profile the potency of inhibitors in a complex mixture of enzymes (Leung et al. 2003). Using this technique, we have generated an inhibitor profile for PREPL<sub>S</sub>. Typical serine protease inhibitors like PMSF and Prefabloc inhibit PREPL completely, as does leupeptin at high concentrations. TPCK, a chymotrypsin inhibitor, and E64, a cysteine protease inhibitor, partially inhibit FP-biotin reactivity. No effect was seen with 4-aminodiphenyl-methanesulfonyl fluoride (APMSF), pepstatin, or EDTA (table 4).

## Discussion

HCS is an autosomal recessive trait characterized mainly by hypotonia, cystinuria, minor facial dysmorphism, and growth hormone deficiency. Molecular analysis has revealed deletions in all patients. In total, four different deletions were identified, ranging from 23.8 kb to 75.8 kb. The smallest region of overlap is 7.7 kb. The coding

sequences of two genes, *SLC3A1* and *PREPL*, are disrupted. Although the deletion of regulatory elements of neighboring genes cannot be entirely excluded, expression studies of the flanking genes, *C2orf34* and *PPM1B*, in an EBV-transformed lymphocyte cell line of one patient with the largest deletion showed the same expression as controls. Comparison with the homozygous 2p21 deletion syndrome (Parvari et al. 2001) shows similar features, such as cystinuria, growth impairment, and hypotonia, although the latter appears to be less severe in HCS. On the other hand, neonatal seizures, severe mental retardation, distinct dysmorphic features, and mitochondrial dysfunction are unique to the 2p21 deletion syndrome and are most likely caused by the absence of the additional genes.

The nine unrelated families live in two small geographic regions. Since only four different deletions were detected, founder effects for deletions A, B, and C were examined using haplotype analysis. Conserved haplotypes flanking the breakpoint were detected in deletions A and C, which extended over at least 1 Mb and 2 Mb, respectively. In patients with deletion B, the conserved haplotype distal to the breakpoint extended over at least 0.7 Mb. Proximal to the breakpoint, two distinct haplotypes are present, most likely because of a crossing-over event shortly after the deletion first appeared. In conclusion, these data support the hypothesis that each of these deletions (A, B, or C) has occurred only once. Their respective ancestral haplotypes are thus still present in our patient group.

The prevalence of microdeletions in this genomic region is hard to estimate. Our observation of two different alleles in a small region of Belgium (Antwerp) and three different deletions in Normandy, France (one of which is also found in Belgian patients), suggests the

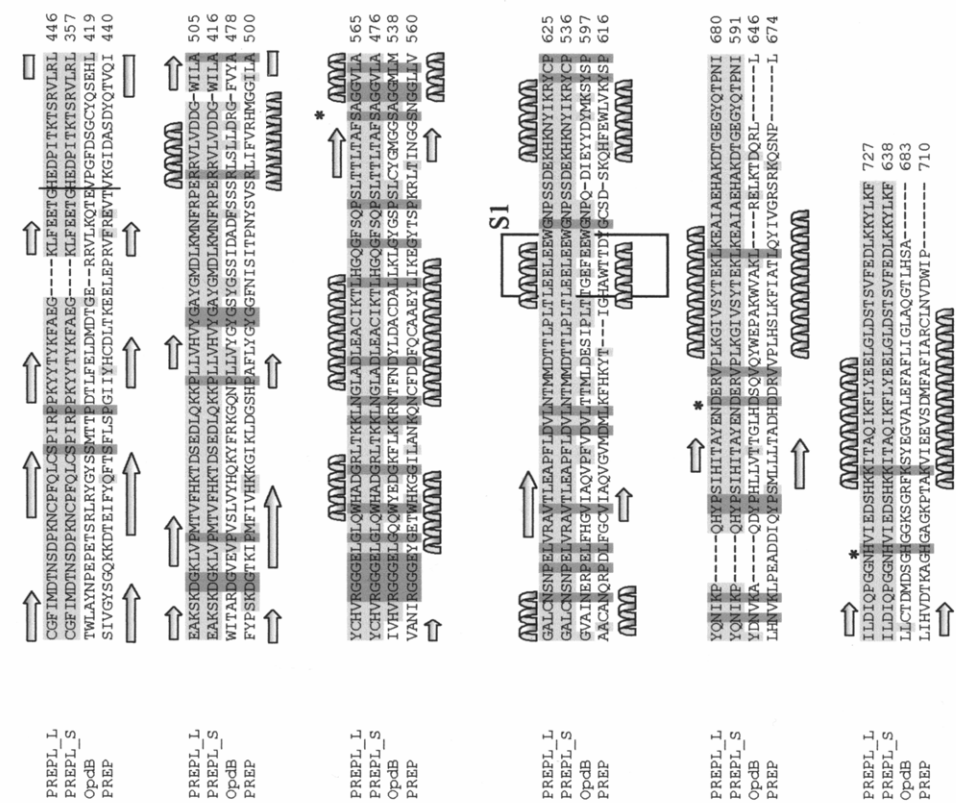


**Figure 5** Multiple sequence alignments of the PREPL variants with PREP and OpdB. Predicted secondary structure elements of the PREPL are shown above the sequence, whereas the PREP secondary structure elements (based on Fulop et al. 1998) are shown below the sequence. Identical residues between PREPL and one homologue are shaded in light gray, whereas completely conserved residues are shaded in dark gray. Catalytic triad residues are indicated by an asterisk, whereas important residues of the S1 binding pocket are boxed.

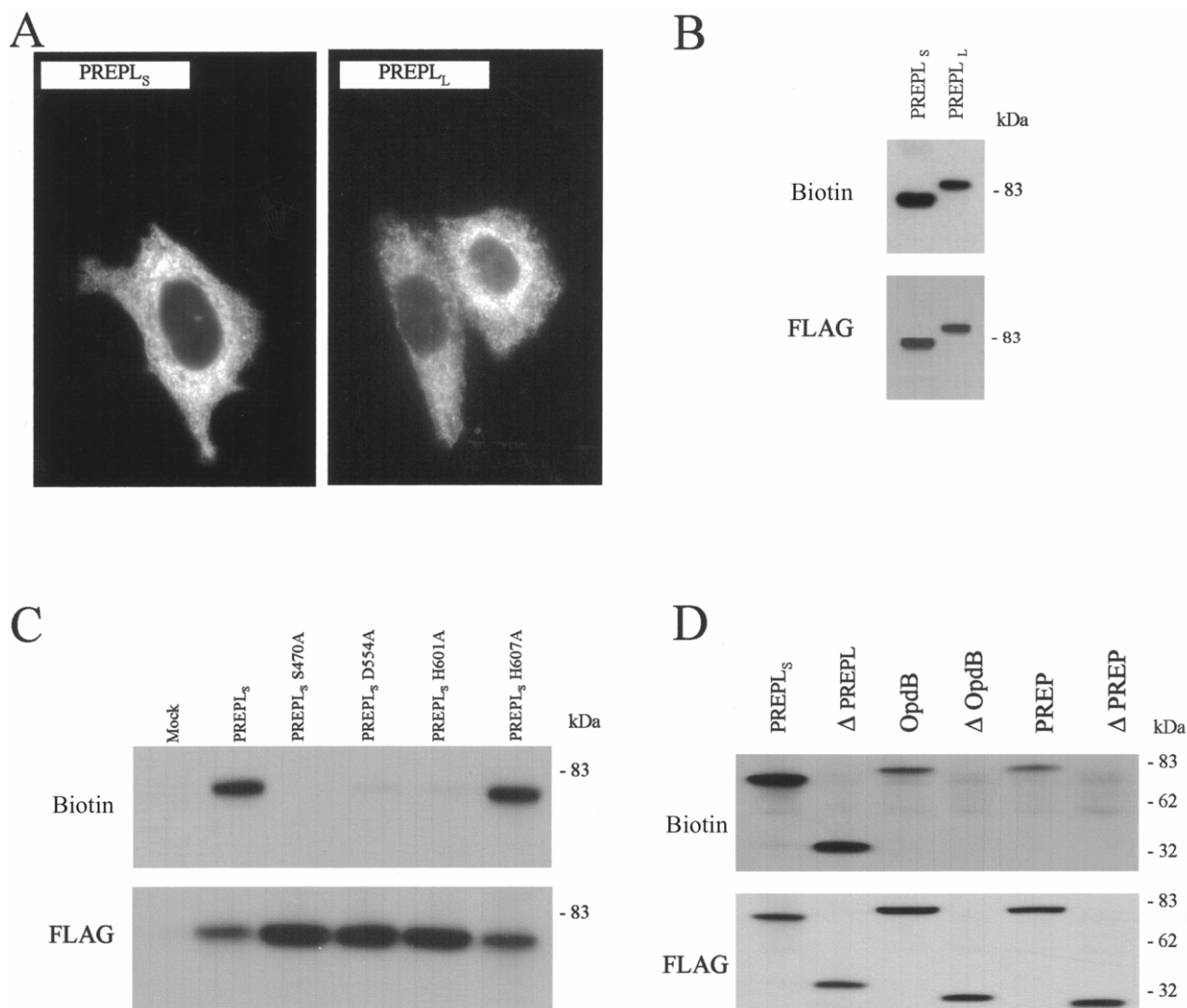


**Figure 6** Functional analysis of PREPL. *A*, Immunofluorescence analysis of PREPL<sub>S</sub> and PREPL<sub>L</sub> in CHO cells. Both isoforms show similar cytoplasmic staining, and similar results were obtained for PREPL<sub>S</sub> when the FLAG epitope was linked to the carboxyterminus instead of to the aminoterminus. *B*, Enzymatic activity of immunopurified, recombinant proteins was determined using FP-biotin and was visualized with streptavidin-HRP. Expression of recombinant proteins was confirmed with biotinylated anti-FLAG M2 antibody. *C*, Wild-type PREPL<sub>S</sub> (lane 2) and mutant His607Ala (lane 6) show reactivity with FP-biotin. In contrast, mutations of the predicted catalytic residues (lanes 3, 4, and 5) ablated activity. *D*, Full-length PREPL<sub>A-B</sub>, OpdB, and PREP are all FP-biotin reactive. Reactivity was abolished in the truncated constructs of OpdB and PREP (lanes 4 and 6) but not in truncated PREPL (lane 2), confirming the fundamental difference in domain structure. ΔPREPL = truncated construct of PREPL (aa 342–638), ΔOpdB = truncated construct of OpdB (aa 405–687), and ΔPREP = truncated construct of PREP (aa 428–710).

prevalence might be relatively high. In addition, three patients who have cystinuria type I with one mutated allele and one deletion of *SLC3A1*, including the 3' UTR (which overlaps with exon 14 of *PREPL*), have been reported but not characterized (Bisceglia et al. 1996; Saadi et al. 1998; Font-Llitjos et al. 2005). A phenotype besides cystinuria type I is not expected, since only one *PREPL* allele is deleted. Furthermore, one sporadic case with similar phenotype has been reported elsewhere (Zaffanello et al. 2003). Molecular diagnosis of

the *SLC3A1/PREPL* locus was suggested but was not performed. It should also be noted that microdeletion of only *PREPL* would result in a phenotype that is much less distinct in the absence of cystinuria and that will, therefore, be more difficult to recognize.

Although the syndrome displays some clinical characteristics (neonatal hypotonia, childhood-onset obesity, short stature, viscous saliva, and hypogenitalism) similar to those seen in PWS, there are striking differences. The neonatal hypotonia described in infants with PWS is

**Table 4****Inhibitor Profile Based on FP-Biotin Reactivity**

Inhibitor <sup>a</sup>	Reactivity (%)	±SD (%)
5-mM PMSF	0	0
1-mM PMSF	14	10
250- $\mu$ M E64	23	6
25- $\mu$ M E64	89	15
1.25-mM TPCK	30	9
250- $\mu$ M TPCK	60	5
6.25-mM Prefabloc	0	0
1.25-mM Prefabloc	10	2
12.5- $\mu$ M APMSF	55	7
12.5- $\mu$ M APMSF	101	14
1.25-mM Leupeptin	4	2
250- $\mu$ M Leupeptin	79	11
12.5-mM EDTA	125	5
12.5- $\mu$ M Pepstatin	75	11

<sup>a</sup> Inhibitors were preincubated with PREPL<sub>s</sub> for 15 min before reaction with FP-biotin.

more severe, with extreme feeding difficulties and the absence of crying. Children with HCS have mild-to-moderate obesity, which is different from the insatiable appetite leading to morbid obesity seen in persons with PWS. Facial dysmorphism is minor in HCS, and the growth of hands and feet is normal. The severe behavioral problems starting during childhood in patients with PWS have not been observed in children with HCS. Hypogonadism is noticed in both syndromes, but, unlike adolescents with PWS, most adolescents with HCS experience a normal pubertal development. In addition, typical PWS symptoms, such as sleeping difficulties, a high threshold for pain or vomiting, and a disturbed thermoregulation, are not observed in persons with HCS.

Since it is well established that mutations in *SLC3A1* cause isolated cystinuria type I, we have focused on characterizing the *PREPL* gene. While this article was in preparation, a study describing the expression and complex splicing of *PREPL*, with similar results, was published (Parvari et al. 2005). *PREPL* is ubiquitously expressed, albeit with much higher expression, in the brain, skeletal muscle, heart, and kidney. Involvement of the brain and skeletal muscle tissues are consistent with the mild mental retardation and hypotonia, whereas no abnormalities (other than cystinuria type I) are observed in heart and kidney tissue. Two groups of transcripts were distinguished: the *PREPL*<sub>1-4</sub> and *PREPL*<sub>5-7</sub> isoforms, which encode 638-aa and 727-aa proteins, respectively. The former group represents the majority of the EST clones and is ubiquitously expressed, whereas the latter is more tissue specific.

PREPL<sub>L</sub> contains 103 aa preceding the  $\beta$ -propeller do-

main, which shares no significant sequence homology with its counterpart in PREP and OpdB. On the other hand, a similar secondary structure is predicted. Unlike PREP and OpdB, however, this subdomain is redundant for FP-biotin reactivity. PREPL also does not appear to contain a sorting signal, since both isoforms are localized in the cytosol. PREPL shares no significant homology with OpdB and PREP in the last 68 aa of the carboxyterminus, although secondary structure predictions suggest that the  $\alpha/\beta$ -hydrolase fold remains intact. Since the crystal structure of PREP demonstrates that those amino- and carboxytermini are in close proximity and are connected through many hydrogen bonds, salt bridges, and hydrophobic interactions, it appears that this subdomain is replaced by a unique subdomain in PREPL, composed only of the carboxyterminal 68 aa. This is consistent with the observation that the most abundant form, PREPL<sub>s</sub>, lacks the aminoterminal subdomain entirely.

The activity of endogenous PREPL (most likely PREPL<sub>s</sub>) in mouse brain by use of FP-biotin was reported elsewhere (Liu et al. 1999). Since no substrates of PREPL have been identified so far, we have used this activity-based probe to identify the catalytic site residues Ser470, Asp554, and His601 and to generate an inhibitor profile. This inhibitor profile strongly suggests that PREPL is a serine protease.

Residues forming the S1 substrate pocket (PREPL<sub>s</sub> E514 and E516) are conserved between PREPL and OpdB, suggesting substrate selectivity for basic residues. Moreover, leupeptin, a peptide-based inhibitor with a P1 arginal group, inhibits the FP-biotin reaction. We have tested this hypothesis with the use of fluorescent substrates and small peptides, but no activity was detected. A prolyl peptidase activity was also ruled out with the use of typical fluorescent PREP substrates. An unbiased approach using degenerate peptide libraries (Turk et al. 2001; Turk and Cantley 2004) did not reveal specific activity (data not shown). This raises the possibility that PREPL has more-stringent substrate requirements than PREP and OpdB, which select almost exclusively on the basis of the P1 amino acid. Determination of the substrate specificity of PREPL will help unveil the molecular mechanism underlying the pathophysiology of HCS.

## Acknowledgments

I. Pauli and A. Vervoort are acknowledged for excellent technical assistance, and Dr. P. van Dijken and Dr. J. Joore are acknowledged for their advice. FP-biotin was synthesized by Dr. W. Dehaen and T. Van Neck. We thank Dr. W. Proesmans and Dr. W. Decaluwé for referring patients, Dr. J. Purroy and colleagues for the initial screening of *SLC3A1* in two patients, and Dr. Annick Vogels for expert opinion on PWS. Grant and scholarship support was provided by the Vlaams Instituut voor

de Bevordering van Wetenschappelijk-Technologisch Onderzoek in de Industrie and the Fonds voor Wetenschappelijk Onderzoek Vlaanderen.

## Web Resources

Accession numbers and URLs for data presented herein are as follows:

BLAST, <http://www.ncbi.nlm.nih.gov/BLAST/>  
ClustalW, <http://www.ebi.ac.uk/clustalw/>  
GDB Human Genome Database, <http://gdbwww.gdb.org/>  
GenBank, <http://www.ncbi.nlm.nih.gov/GenBank/> (for full-length human *PREPL<sub>S</sub>* cDNA [accession number AB007896], full-length human *PREPL<sub>C</sub>* cDNA [accession number AK131463], full-length *E. coli* *OpdB* cDNA sequence [accession number U00096], and full-length human *PREP* sequence [accession number NM002726])  
Jpred, <http://www.compbio.dundee.ac.uk/~www-jpred/>  
Online Medelian Inheritance in Man (OMIM), <http://www.ncbi.nlm.nih.gov/Omim/> (for *PREP*, *OpdB*, *DPPIV*, *APEH*, 2p21 deletion syndrome, and isolated cystinuria type I)  
PredictProtein, <http://www.embl-heidelberg.de/predictprotein/>  
Primer3, [http://frodo.wi.mit.edu/cgi-bin/primer3/primer3\\_www.cgi/](http://frodo.wi.mit.edu/cgi-bin/primer3/primer3_www.cgi/)  
PSORT II, <http://psort.nibb.ac.jp/form2.html/>

## References

- Berger A, Schechter I (1970) Mapping the active site of papain with the aid of peptide substrates and inhibitors. *Philos Trans R Soc Lond B Biol Sci* 257:249–264
- Bisceglia L, Calonge MJ, Dello Strologo L, Rizzoni G, de Sanctis L, Gallucci M, Beccia E, Testar X, Zorzano A, Estivill X, Zelante L, Palacin M, Gasparini P, Nunes V (1996) Molecular analysis of the cystinuria disease gene: identification of four new mutations, one large deletion, and one polymorphism. *Hum Genet* 98:447–451
- Buiting K, Dittrich B, Gross S, Lich C, Farber C, Buchholz T, Smith E, et al (1998) Sporadic imprinting defects in Prader-Willi syndrome and Angelman syndrome: implications for imprint-switch models, genetic counseling, and prenatal diagnosis. *Am J Hum Genet* 63:170–180
- Burleigh BA, Caler EV, Webster P, Andrews NW (1997) A cytosolic serine endopeptidase from *Trypanosoma cruzi* is required for the generation of Ca<sup>2+</sup> signaling in mammalian cells. *J Cell Biol* 136:609–620
- Caler EV, Morty RE, Burleigh BA, Andrews NW (2000) Dual role of signaling pathways leading to Ca(2+) and cyclic AMP elevation in host cell invasion by *Trypanosoma cruzi*. *Infect Immun* 68:6602–6610
- Caler EV, Vaena de Avalos S, Haynes PA, Andrews NW, Burleigh BA (1998) Oligopeptidase B-dependent signaling mediates host cell invasion by *Trypanosoma cruzi*. *Embo J* 17:4975–4986
- Calonge MJ, Gasparini P, Chillaron J, Chillon M, Gallucci M, Rousaud F, Zelante L, Testar X, Dallapiccola B, Di Silverio F, Barcelo P, Estivill X, Zorzano A, Nunes V, Palacin M (1994) Cystinuria caused by mutations in rBAT, a gene involved in the transport of cystine. *Nat Genet* 6:420–425
- Clara R, Lowenthal A (1966) Familial aminoaciduria with muscular hypotonia and dwarfism. *Bull Acad R Med Belg* 6:577–611
- Creemers JW, Usac EF, Bright NA, Van de Loo JW, Jansen E, Van de Ven WJ, Hutton JC (1996) Identification of a transferable sorting domain for the regulated pathway in the prohormone convertase PC2. *J Biol Chem* 271:25284–25291
- Creemers JW, van de Loo JW, Plets E, Hendershot LM, Van De Ven WJ (2000) Binding of BiP to the processing enzyme lymphoma pro-
- protein convertase prevents aggregation, but slows down maturation. *J Biol Chem* 275:38842–38847
- Drucker DJ (2001) Minireview: the glucagon-like peptides. *Endocrinology* 142:521–527
- Font-Llitjos M, Jimenez-Vidal M, Bisceglia L, Di Perna M, de Sanctis L, Rousaud F, Zelante L, Palacin M, Nunes V (2005) New insights into cystinuria: 40 new mutations, genotype-phenotype correlation, and digenic inheritance causing partial phenotype. *J Med Genet* 42:58–68
- Fulop V, Bocskai Z, Polgar L (1998) Prolyl oligopeptidase: an unusual beta-propeller domain regulates proteolysis. *Cell* 94:161–170
- Fulop V, Szeltner Z, Polgar L (2000) Catalysis of serine oligopeptidases is controlled by a gating filter mechanism. *EMBO Rep* 1:277–281
- Gerczei T, Keseru GM, Naray-Szabo G (2000) Construction of a 3D model of oligopeptidase B, a potential processing enzyme in prokaryotes. *J Mol Graph Model* 18:7–17, 57–18
- Goodyer P, Boutros M, Rozen R (2000) The molecular basis of cystinuria: an update. *Exp Nephrol* 8:123–127
- Jackson RS, Creemers JW, Farooqi IS, Raffin-Sanson ML, Varro A, Dockray GJ, Holst JJ, Brubaker PL, Corvol P, Polonsky KS, Ostrega D, Becker KL, Bertagna X, Hutton JC, White A, Dattani MT, Hussain K, Middleton SJ, Nicole TM, Milla PJ, Lindley KJ, O'Rahilly S (2003) Small-intestinal dysfunction accompanies the complex endocrinopathy of human proprotein convertase 1 deficiency. *J Clin Invest* 112:1550–1560
- Juhasz T, Szeltner Z, Fulop V, Polgar L (2005) Unclosed beta-propellers display stable structures: implications for substrate access to the active site of prolyl oligopeptidase. *J Mol Biol* 346:907–917
- Kikuno R, Nagase T, Nakayama M, Koga H, Okazaki N, Nakajima D, Ohara O (2004) HUGE: a database for human KIAA proteins, a 2004 update integrating HUGEppi and ROUGE. *Nucleic Acids Res* 32:D502–D504
- Leung D, Hardouin C, Boger DL, Cravatt BF (2003) Discovering potent and selective reversible inhibitors of enzymes in complex proteomes. *Nat Biotechnol* 21:687–691
- Liu Y, Patricelli MP, Cravatt BF (1999) Activity-based protein profiling: the serine hydrolases. *Proc Natl Acad Sci USA* 96:14694–14699
- Maes M, Goossens F, Scharpe S, Calabrese J, Desnyder R, Meltzer HY (1995) Alterations in plasma prolyl endopeptidase activity in depression, mania, and schizophrenia: effects of antidepressants, mood stabilizers, and antipsychotic drugs. *Psychiatry Res* 58:217–225
- Maes M, Goossens F, Scharpe S, Meltzer HY, D'Hondt P, Cosyns P (1994) Lower serum prolyl endopeptidase enzyme activity in major depression: further evidence that peptidases play a role in the pathophysiology of depression. *Biol Psychiatry* 35:545–552
- Morty RE, Fulop V, Andrews NW (2002) Substrate recognition properties of oligopeptidase B from *Salmonella enterica* serovar Typhimurium. *J Bacteriol* 184:3329–3337
- Nardini M, Dijkstra BW (1999) Alpha/beta hydrolase fold enzymes: the family keeps growing. *Curr Opin Struct Biol* 9:732–737
- Ollis DL, Cheah E, Cygler M, Dijkstra B, Frolow F, Franken SM, Harel M, Remington SJ, Silman I, Schrag J, Sussman JL, Verschuere KHG, Goldman A (1992) The alpha/beta hydrolase fold. *Protein Eng* 5:197–211
- Parvari R, Brodyansky I, Elpeleg O, Moses S, Landau D, Hershkovitz E (2001) A recessive contiguous gene deletion of chromosome 2p16 associated with cystinuria and a mitochondrial disease. *Am J Hum Genet* 69:869–875
- Parvari R, Gonen Y, Alshafee I, Buriakovsky S, Regev K, Hershkovitz E (2005) The 2p21 deletion syndrome: characterization of the transcription content. *Genomics* 86:195–211
- Polgar L (2002) The prolyl oligopeptidase family. *Cell Mol Life Sci* 59:349–362
- Purroy J, Bisceglia L, Jaeken J, Gasparini P, Palacin M, Nunes V (2000)

- Detection of two novel large deletions in SLC3A1 by semi-quantitative fluorescent multiplex PCR. *Hum Mutat* 15:373–379
- Rawlings ND, Barrett AJ (1994) Families of serine peptidases. *Methods Enzymol* 244:19–61
- Roebroek AJ, Taylor NA, Louagie E, Pauli I, Smeijers L, Snellinx A, Lauwers A, Van de Ven WJ, Hartmann D, Creemers JW (2004) Limited redundancy of the proprotein convertase furin in mouse liver. *J Biol Chem* 279:53442–53450
- Saadi I, Chen XZ, Hediger M, Ong P, Pereira P, Goodyer P, Rozen R (1998) Molecular genetics of cystinuria: mutation analysis of SLC3A1 and evidence for another gene in type I (silent) phenotype. *Kidney Int* 54:48–55
- Scaloni A, Jones W, Pospischil M, Sassa S, Schneewind O, Popowicz AM, Bossa F, Graziano SL, Manning JM (1992) Deficiency of acyl-peptide hydrolase in small-cell lung carcinoma cell lines. *J Lab Clin Med* 120:546–552
- Schulz I, Gerhartz B, Neubauer A, Holloschi A, Heiser U, Hafner M, Demuth HU (2002) Modulation of inositol 1,4,5-triphosphate concentration by prolyl endopeptidase inhibition. *Eur J Biochem* 269: 5813–5820
- Szeltner Z, Renner V, Polgar L (2000) Substrate- and pH-dependent contribution of oxyanion binding site to the catalysis of prolyl oligopeptidase, a paradigm of the serine oligopeptidase family. *Protein Sci* 9:353–360
- Turk BE, Cantley LC (2004) Using peptide libraries to identify optimal cleavage motifs for proteolytic enzymes. *Methods* 32:398–405
- Turk BE, Huang LL, Piro ET, Cantley LC (2001) Determination of protease cleavage site motifs using mixture-based oriented peptide libraries. *Nat Biotechnol* 19:661–667
- Vilsboll T, Krarup T, Deacon CF, Madsbad S, Holst JJ (2001) Reduced postprandial concentrations of intact biologically active glucagon-like peptide 1 in type 2 diabetic patients. *Diabetes* 50:609–613
- Williams RS, Cheng L, Mudge AW, Harwood AJ (2002) A common mechanism of action for three mood-stabilizing drugs. *Nature* 417: 292–295
- Williams RS, Eames M, Ryves WJ, Viggars J, Harwood AJ (1999) Loss of a prolyl oligopeptidase confers resistance to lithium by elevation of inositol (1,4,5) trisphosphate. *Embo J* 18:2734–2745
- Yoshimoto T, Ogita K, Walter R, Koida M, Tsuru D (1979) Post-proline cleaving enzyme: synthesis of a new fluorogenic substrate and distribution of the endopeptidase in rat tissues and body fluids of man. *Biochim Biophys Acta* 569:184–192
- Zaffanello M, Beghini R, Zamboni G, Fanos V (2003) A sporadic case of cystinuria, respiratory chain and growth hormone deficiencies. *Pediatr Nephrol* 18:846–847